Rotating Bending Fatigue Tests of PH-42 steel Plasma Nitrided

José Divo Bressan[1,*], Daniel Kohls[2]

[1] Department of Mechanical Engineering, Center for Technological Sciences, University of Santa Catarina State, Campus Universitário, 89.223-100 Joinville, Santa Catarina, Brazil.
[2] Faculty of EEFF, Institute of GGHH, City Post Code, Country
* Corresponding author: dem2jdb@joinville.udesc.br

Abstract: The aim of this study was to evaluate the influence of plasma nitriding process on the fatigue limit of PH-42 Supra steel provided by Schmolz + Bickenbach of Brazil. The paper presents the experimental results of rotating bending fatigue tests for specimens as received and treated by plasma nitriding process with a nitrided layer of 0.3mm. This material is employed in manufacturing polymer injection molds and inserts, and offers high hardness and good machinability. The fatigue tests were carried out by a rotating bending fatigue machine which allowed to plot and compare the Wöhler's curve for both types of steel specimens. Moreover, the hardness of the nitrided layer and substrate, the hardness of the non-nitrided specimens, the ultimate strength from simple tensile tests were determined experimentally. The fatigue testing results were used to obtain the material empirical Basquin's fatigue life equations. Photographs by SEM of the fractured surface were obtained and provided a visual aspect analysis of nitrided and non-nitrided specimens in tensile and fatigue testing. The fatigue limit stress increased from 440 MPa to 710 MPa for non nitrided and plasma nitrided PH-42 steel respectively. In addition, the fatigue limit behavior and fracture mechanisms, depending on the application of advanced plasma nitrided layer, are also discussed.

Keywords: PH-42 steel, rotating bending test, plasma nitriding, fatigue limit.

1. Introduction

Rupture in a structural or mechanical component frequently initiate at metal surface under two loading conditions, owing to metal fatigue process. Firstly, it is related to high loading cycles of component, leading to resultant stresses greater than the material fatigue limit. Under this type of high loading, rupture occur at shorter number of cycles due to the inception of surface micro-cracks which are originated from shear bands in preferential sliding atomic planes and directions in the material.

Secondly, there are situations of fracture occurring in components due to surface crack nucleation which are originated from surface defects such as grooves, scratches, pores, holes or metallic inclusions, even for low stresses. However, fatigue cracks can also be originated from non-metallic inclusions and defects situated in sub-layers just below the component surface [1]. This kind of rupture has been referred in literature to explain the behavior of high strength steels. In surface treated steels, fatigue limit is expected to increase proportionally to hardness increase. However, it is worth to recall that for steels with hardness above 400 Vickers there is a reduction of fatigue limit which is related to non-metallic inclusions. This can be observed in Fig. 1, showing the fatigue limit of various steel grades versus hardness [2]: fatigue limit increases up to a maximum and then falls with increasing hardness.

Moreover, there are other issues related to fatigue resistance of steels such as the presence of profile of residual stresses near the surface site of crack nucleation due to machining and shot peening processes [3].

In metal fatigue, tensile stresses act to open crack tip and promotes crack growth. However, compressible stresses can increase the fatigue limit or have little or no contribution to crack generation and propagation. In this context, it is important to study the fatigue limit of machined steel components of high hardness and steel components with plasma nitriding surface treatment which increase even more the surface hardness.

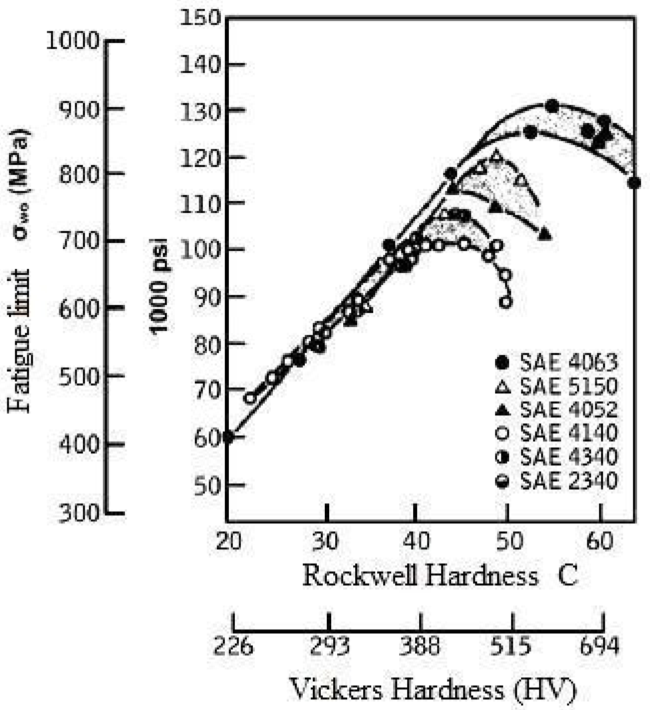

Figure 1. Fatigue limit of various steel grades versus hardness [2].

Hence, the main goal of this work is to present and compare the experimental results of rotating bending fatigue tests of PH-42 Supra steel plasma nitrided and non-nitrided which is low carbon steel and are employed to fabricate plastic injection molds and inserts.

2. Material and Experimental Procedure

Fatigue tests were performed using specimens of PH-42 Supra steel delivered by Schmolz + Bickenbach of Brazil. According to the steel supplier, the material had limit strength of 1250 MPa, elasticity modulus of 206 GPa and Rockwell hardness of 40HRC [4]. For the plasma nitrided steel specimens the attained surface hardness was 60HRC. The material chemical composition is shown in Table 1.

Table 1. Chemical composition of PH-42 Supra steel, according to supplier [5].

C %	Mg %	Ni %	Cu %	Al %
0.15	1.5	3.0	1.0	1.0

25 fatigue test specimens as received (non-nitrided) and 25 plasma nitrided specimens with a nitriding layer of 0.3mm, were tested in a rotating bending fatigue machine and the results were plotted and compared by Wöhler's curve for both types of steel specimens. Besides, the surface hardness of non-nitrided and plasma nitrided specimens and the limit strength were obtained by hardness and tensile tests respectively. Photographs by SEM of the fractured surface specimens were obtained and provided a visual analysis of fracture of nitrided and non-nitrided specimens in tensile and fatigue tests.

The fatigue test specimens were machined from one bar, according to the dimensions seen in Fig.2. Each specimen were polished to surface average roughness of Ra = 0.11μm in the useful region which had lower specimen diameter of 7.0mm.

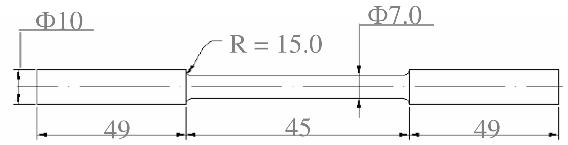

Figure 2. Geometry dimensions of rotating bending fatigue test specimens.

Figure 3 shows a photo of a non-nitrided specimen employed in the rotating bending fatigue test which attained a fatigue life over 10^6 cycles.

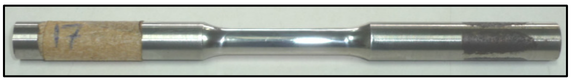

Figure 3. Photo of a rotating bending fatigue test specimen which attained fatigue life over 10^6 cycles.

2.1. Fatigue Tests

Fatigue tests were carried out in the rotating bending fatigue machine, type TYP RM 506, Budapeste/Hungary, seen in Fig. 4. The specimen bending load was applied by a load arm existing in the machine. The true bending load applied on the fatigue specimen corresponds to 10 times the load applied on the plate situated at the opposite arm end.

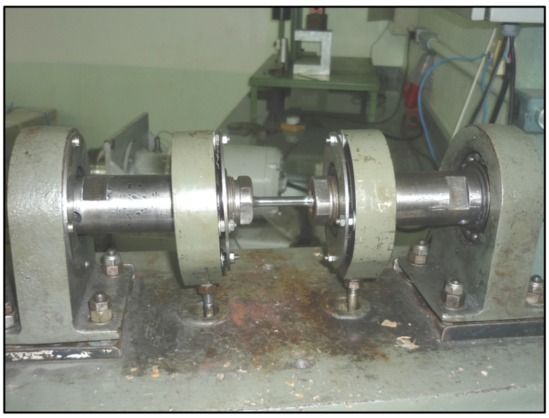

Figure 4. Photo of the rotating bending fatigue machine, type TYP RM 506, utilized in the fatigue tests.

Hence, the tensile and compression stresses on the specimen surface were calculated by the equation,

$$\sigma = 160 \frac{Pa}{\pi D^3} \quad (\text{kgf/mm}^2) \tag{1}$$

where D (= 7mm) is the diameter of the useful region in the specimen, P (kgf) is the applied load on the plate at the load arm end and "a" is the distance from the point of bending support (ball bearing) to the point of load application. For the nitrided specimens, the load varied from 4.8 to 8.0kgf and for non-nitrided specimens the load varied from 2.72 to 5.2kgf. The electric motor rotating velocity was fixed and equal to 3000 rpm.

The fatigue tests were initiated for high applied load until the specimen rupture. This high load was gradually reduced for the following specimens till obtaining the fatigue limit for the material. The fatigue limit was defined as the maximum stress for fatigue life of 10^6 cycles.

3. Results and Discussions

3.1. Vickers Micro-Hardness

Tables 2 and 3 shows the average Vickers micro-hardness (mHV), using indenter load of 500g, for the PH-42 Supra steel fatigue specimen plasma nitrided at two distinct regions: measured on the plasma nitrided surface layer of 0.3mm, Table 2, and at the substrate or bulk of material, Table 3. In addition, the correspondent Rockwell C hardness conversion is also presented. In Table 4, the average Vickers micro-hardness measured at surface, indenter load of 500g, for the non-nitrided specimen of PH-42 Supra steel fatigue specimen is presented. The nitriding process has increased the substrate material hardness from 454 to 885 mHV as can be observed from Table 3 and 4.

Table 2. Vickers micro-hardness of nitrided surface layer of PH-42 Supra steel nitrided specimen.

Load 500g	Vickers micro-hardness (mHV0.5)	Conversion to Rockwell C hardness (HRC)
	861.22	65.9
	900.56	67.0
	893.77	66.8
Average	885.2	66.6

Table 3. Vickers micro-hardness of substrate of PH-42 Supra steel nitrided specimen.

Load 500g	Vickers micro-hardness (mHV0.5)	Conversion to Rockwell C hardness (HRC)
	680.41	59.2
	588.70	54.6
	599.54	55.2
	727.31	61.2
Average	648.99	57.7

Table 4. Vickers micro-hardness of PH-42 Supra steel non-nitrided specimen.

Load 500g	Vickers micro-hardness (mHV0.5)	Conversion to Rockwell C hardness (HRC)
	446.0	45.0
	434.0	44.0
	484.0	48.0
	506.0	45.6
Average	454.2	45.6

3.2. Surface Roughness

Before fatigue tests, the arithmetic average surface roughness Ra of plasma nitrided and non-nitrided specimens were measured, utilizing a profilometer Supertronic 25 Taylor Robson, with total sliding distance of 4.0mm and Gausian filter of 0.8mm [5]. The experimental results for three specimens and total average Ra are presented in Table 6 for 10 measurements on each specimen. The plasma nitrided specimens have increased the surface roughness Ra in relation to the non-nitrided specimens, but they both can be considered polished for their very low values. This is due to the formation of precipitates and nitrides on the nitriding layer [6].

Table 7. Arithmetic average surface roughness Ra of plasma nitrided and non-nitrided specimens.

Specimen	Ra (μm) Plasma nitrided	Ra (μm) non-nitrided
1	0.31	0.14
2	0.44	0.11
3	0.29	0.08
Total average	0.35	0.11

3.2. Rotating Bending Fatigue Test Results

The fatigue limits for as received (non-nitrided) and plasma nitrided specimens were obtained directly from the plotted Wöhler's curve, seen in Fig. 5, which is the curve of fatigue life for the alternate bending stress tests versus total number of cycles to specimen fracture [7]. According to ASTM E466 standard recommendation, fatigue limit correspond to the maximum rupture stress for the number of cycles equal or superior to 10^6 cycles. The average values are presented in Table 5.

Table 5. Fatigue Limit Stress for PH-42 Supra steel specimens plasma nitrided and non-nitrided. Average values obtained from the plotted Wöhler's curve for fatigue life (1kgf/mm^2 ≅ 10 MPa).

Specimen	Fatigue Limit Stress σ_{fad} (MPa)
Ph-42 Supra steel plasma nitrided	710.0
Ph-42 Supra steel non-nitrided	440.0

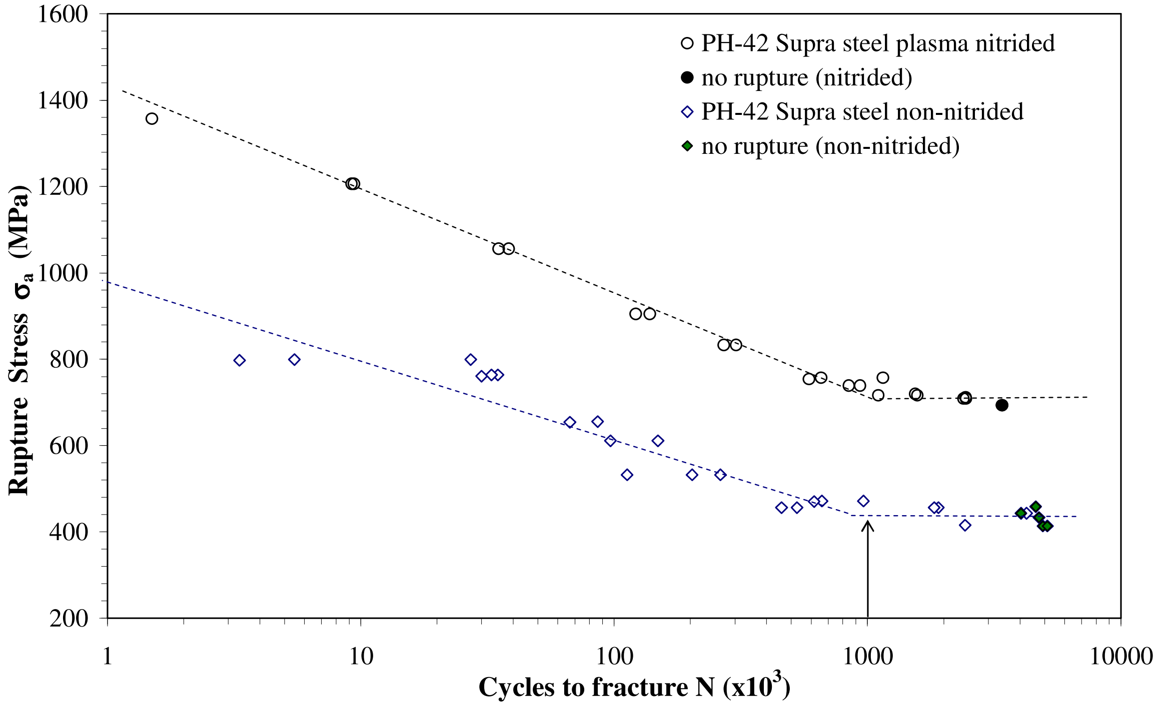

Figure 5. Stress versus number of cylces N to fracture curves for rotating bending fatigue test for PH-42 Supra steel non-nitrided and plasma nitrided with layer of 0.3mm. Fatigue limit is for $N=10^6$ cycles.

In Fig. 6, some fractured non-nitrided specimens after the rotating bending fatigue tests can be observed which fracture site is similar to the plasma nitrided specimens.

Figure 6. Photo of three non-nitrided specimens after the fatigue test.

3.3. Tensile Tests

Tensile tests were also performed, using the same fatigue test specimens of PH-42 Supra steel plasma nitrided with nitriding layer of 0.3mm and non-nitrided as seen in Fig. 2. The ultimate tensile strength values are shown in Table 6.

Table 6. Ultimate tensile strength obtained experimentaly from tensile tests.

Sperimen	Ultimate tensile strength σ_t (MPa)
Ph-42 Supra steel plasma nitrided	1174.3
Ph-42 Supra steel non-nitrided	1150.0

3.4. Basquin's Equation

The empiric law of Basquin for fatigue life [8] of PH-42 Supra steel plasma nitrided specimens obtained from the plotted mean curve in Fig. 5 is given by,

$$\sigma_a = 2921\ N_f^{-0.1024}\ \text{(MPa)} \tag{2}$$

and for PH-42 Supra steel non-nitrided specimens, the Basquin's equation is given by,

$$\sigma_a = 2182.7\ N_f^{-0.1159}\ \text{(MPa)} \tag{3}$$

where σ_a is the bending cyclic stress amplitude and N_f is the number of cycles to rupture.

3.5. Fractograph by SEM

Fracture surface by SEM of PH-42 Supra steel plasma nitrided tensile test specimens are shown in Fig. 7a and 7b. Surface cracks initiated in the nitrided layer and at 90 degree to the load line are seen. Hence, the fracture mechanism of the nitrided layer was brittle fracture due to principal maximum tensile stress. The measured plasma nitrided layer thickness was 337.87μm.

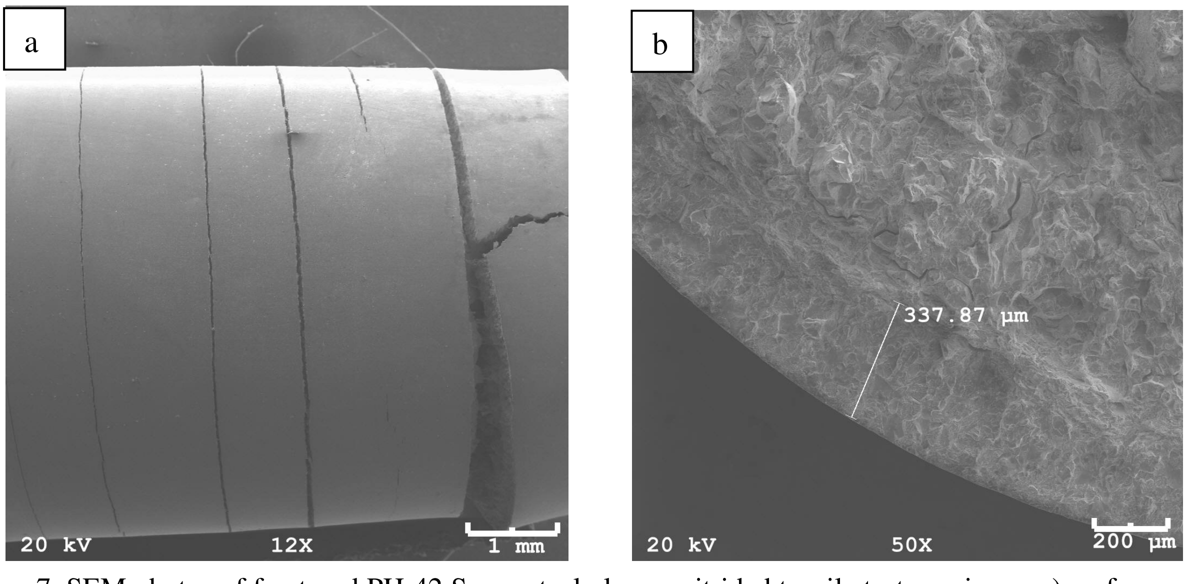

Figure 7. SEM photos of fractured PH-42 Supra steel plasma nitrided tensile test specimen: a) surface cracks and b) fracture surface showing the plasma nitrided layer thickness of 337.87μm.

In Fig. 8, fracture surface of fatigue test specimen of PH-42 Supra steel non-nitrided are presented. Brittle fracture mechanism in Fig. 8a and 8b and the fatigue crack length near the specimen surface can be observed. In Fig. 9a and 9b, fracture surface of fatigue test specimen of PH-42 Supra steel plasma nitrided are shown. Instantaneous rupture by brittle fracture and a very small fatigue region near specimen surface are seen. The fatigue crack length near the specimen surface can be evaluated in Fig. 9b, approximately 20μm owing to plastic compressive deformations.

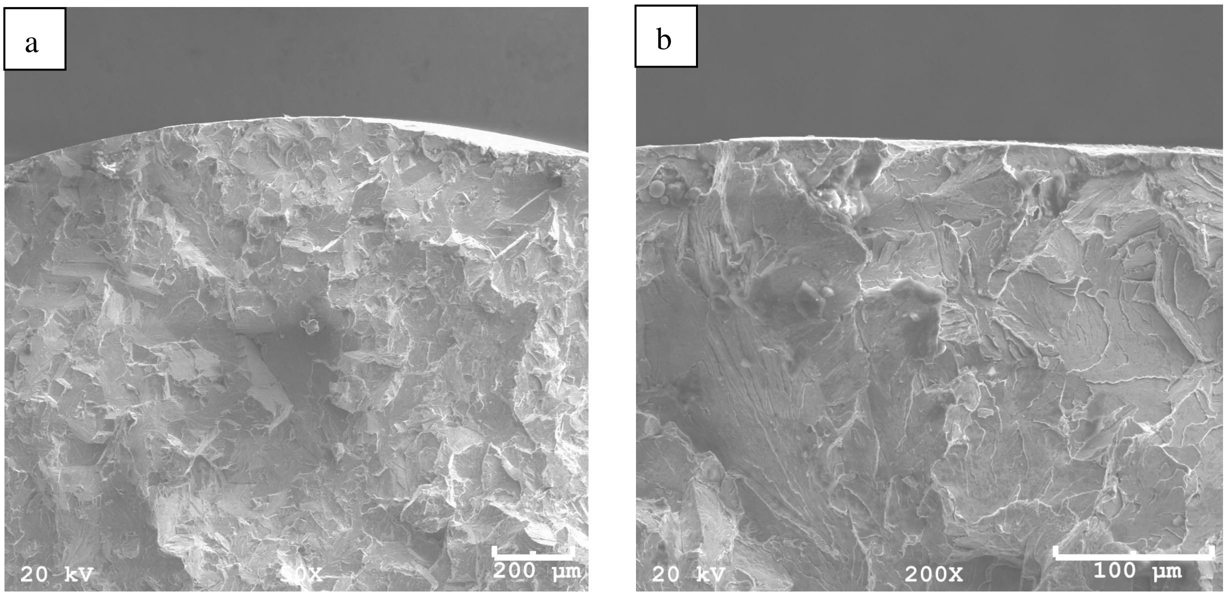

Figure 8. SEM photos of fracture surface of PH-42 Supra steel non-nitrided fatigue test specimen in rotating bending test: a) rupture by brittle fracture and b) detail of beginning of fatigue crack at specimen surface.

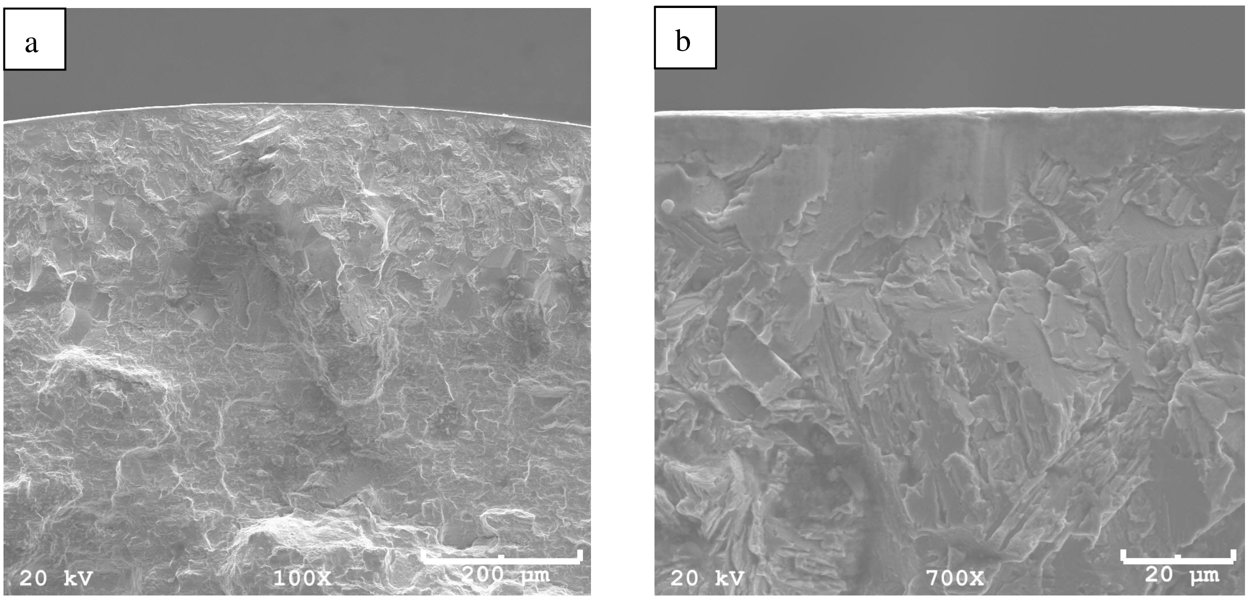

Figure 9. SEM photos of fracture surface of PH-42 Supra steel plasma nitrided fatigue test specimen in rotating bending test: a) rupture by brittle fracture and b) detail of fatigue crack growth at specimen surface.

4. Conclusions

From the experimental results of PH-42 Supra steel (Schmolz + Bickenbach do Brasil) plasma nitrided, nitriding layer of 0.3mm, and as received (non-nitrided) specimens tested in tensile test, Vickers micro-hardness and rotating bending fatigue testing and analysis of fracture surface by SEM, the following conclusion can be drawn,

a) Fatigue limit stress of PH-42 Supra steel plasma nitrided was 710 MPa which is much higher than the bulk material or non-nitrided specimen of 440 MPa. Hence, the plasma nitriding process has increased the fatigue limit stress by 61%.

b) The plasma nitriding process has increased the material hardness from 454 to 885 mHV.

c) Basquin's empiric law for fatigue life of PH-42 Supra steel plasma nitrided specimens was $\sigma_a = 2921\ N_f^{-0.1024}$ (MPa) and for non-nitrided specimens, $\sigma_a = 2182.7\ N_f^{-0.1159}$ (MPa).

d) SEM analysis of fracture surface of fatigue test specimen of PH-42 Supra steel non-nitrided presented brittle fracture mechanism: the fatigue crack length near the surface was very small.

e) SEM analysis of fracture surface of fatigue test specimen of PH-42 Supra steel plasma nitrided had shown rupture by brittle fracture and a very small fatigue region near specimen surface. The fatigue crack length near the specimen surface was evaluated approximately 20μm owing to plastic compressive deformations.

f) The plasma nitrided specimens have increased the surface roughness Ra in relation to the non-nitrided specimens from Ra = 0.11μm to 0.35μm for non-nitrided and plasma nitrided respectively, but they both can be considered polished for their very low values.

g) In tensile tests, surface cracks initiated in the nitrided layer and at 90 degree to the load line are seen. Hence, the fracture mechanism of the nitrided layer in tensile test was brittle fracture due to principal maximum tensile stress.

Acknowledgements

The authors would like to thank the company TOX Pressotechnik of Joinville/Brazil for providing the specimens, University of Santa Catarina State and CNPq of Brazil for financial support.

References

[1] C.E.S. Amorim, Análise dos recobrimentos anticorrosivos aplicados sobre um aço aeronáutico de alta resistência no comportamento em fadiga. Thesis (Doutoramento in Mechanical Engineering), Faculdade de Engenharia de Guaratinguetá, Guaratinguetá/Brazil, 2003.

[2] Y. Murakami; S. Kodama; S. Konuma, Quantitative evaluation of effects of non-metallic inclusions on fatigue strength steels I: Basic fatigue mechanism and evaluation of correlation between fracture stress and the size and location of nonmetallic inclusions. Int. J. Fatigue, Sept. (1989) 291-298.

[3] H.J.C. Voorvald; M.P. Silva; M.Y.P. Costa; M.O.H. Cioffi, Improvement in the fatigue strength of chromium electroplated AISI 4340 steel by shot peening. Fatigue &Structures, 32 (2009) 97-104.

[4] Formadur PH-42 Superclean. Available in http://www.schmolz-bickenbach.com.br/fileadmin/files/schmolz-bickenbach.com.br/documents/Fichas_Tecnicas_novo_formato_dez2011/Moldes/Formadur_Ph42superclean.pdf> acessed on 4 december 2011.

[5] Rebrac Instrumentos de Medição, Rugosidade. Available in <http://www.rebrac.com.br/downloads/RUGOSIDADE%20-par%C3%A2metros-.pdf>. acessed on april 2011.

[6] Análise da rugosidade e Microestrutura de Camadas Nitretadas Obtidas pelos Processos Líquido, Gasoso e Iônico em Aço AISI H13. Available in <http://www.bodycote.com.br/artigos/artigoNitretacao.pdf> acessed on 23 april 2011.

[7] S.A. Meguid, Engineering Fracture Mechanics. Department of Mechanical Engineering, University of Toronto, Canada, Elsevier Applied Science, 1989, p. 75-79.

[8] Norman E. Dowling, Mechanical Behavior of Materials. 3rd edition, Prentice-Hall, USA, 2006.